

Synthesis and CO₂ Absorption of Anhydrous Colloidal Suspension Based on Hollow Silica Nanospheres

Yudong Ding*, Liheng Guo, Xiaoqiang Li, Qiang Liao, Xun Zhu, Hong Wang

Chongqing Univ., Key Laboratory of Low-grade Energy Utilization Technologies and Systems, Shazheng St.174, Shapingba Dist., Chongqing 400030, China
 dingyudong@cqu.edu.cn

A novel anhydrous colloidal suspension was synthesized experimentally for CO₂ absorption by dispersing hollow silica nanospheres (HSNs) modified by diethylenetriamine (DETA) in 2-[2-(dimethylamine) ethoxy] ethanol (DMEE) in this work. The physicochemical properties of HSNs synthesized were studied, and HSNs presented uniformed sphere-like morphology and microporous structures dominated by micropores. The CO₂ absorption performance of DETA-HSNs/DMEE with different DETA loading contents (0 - 60 wt%) was investigated. A high DETA loading content can promote effectively the CO₂ absorption capacity, and 60 wt%DETA-HSNs/DMEE had a highest absorption capacity of 1.0630 ± 0.0849 mmol/g. But more DETA resulted into a greater resistance of CO₂ transfer in the late stage of absorption, and extend the absorption time. Moreover, pseudo-second-order model could be more successful to predict the CO₂ absorption process in the colloidal suspensions studied.

1. Introduction

The greenhouse effect caused by a large amount of carbon dioxide emission has posed a serious threat to the human environment and survival, and attracted worldwide attention. To effectively reduce carbon dioxide emission, CO₂ capture and storage (CCS) is still identified as a vital approach in CO₂ emission mitigation in the foreseeable future (IEA, 2017).

For CO₂ capture technology, efficient and economical carbon dioxide capture material plays an important role. Various types of materials have been developed and studied. Organic amine solution is a kind of common liquid absorbent, especially monoethanolamine (MEA) solution, which has many advantages such as high absorption amount and fast absorption rate (Ling et al., 2019). Many new liquid absorbents are synthesized and studied in recent years, such as mixed amine solution (Mehassouel et al., 2016) and amino functionalized ionic liquids (Amir et al., 2018). Considering the low regeneration energy consumption, wide range of operating temperature and other advantages, solid porous adsorbents have also attracted the attention of researchers (Nie et al., 2018), such as zeolite, metallic oxides, and metal organic frameworks (MOFs), and so on. Based on a broad range of experimental data, Dashti et al. (2018) compared and evaluated four different computing techniques to predict gas adsorption on zeolite-5A. Amine functionalized mesoporous silica were synthesized and the effects of pore structure, types of amines and cycle performance on CO₂ adsorption measurements were conducted (Jiao et al., 2016). However, for solid adsorption materials, cyclic utilization and large-scale continuous operation are difficult.

To combine the fluidity of liquid absorbent and the excellent characteristics of solid adsorbent for CO₂ capture, an anhydrous colloidal suspension as a sorbent was prepared by suspending hollow silica nanospheres modified by amino in DMEE in this work. A simple synthetic method and cheap raw materials can ensure the good economy. DMEE, a nonaqueous solvent with good liquidity, can avoid evaporation heat to reduce energy consumption, and facilitate system integration to recover heat. The physicochemical properties of hollow silica nanospheres and the absorption performance of CO₂ in the colloidal suspension were characterized and analysed. The effect of DETA loading content on absorption performance was studied. In addition, absorption kinetic models for CO₂ transfer process in the suspension absorbents were analyzed.

2. Experiment

2.1 Preparation of DETA-HSNs/DMEE

In a typical synthesis, prepared polystyrene (PS) emulsion (10 g) containing 4 g powders was added into the mixed solution of methanol (45 mL) and deionized water (24 mL). After ultrasonic dispersion (frequency of 40 kHz, power of 180 W) for 30 minutes, the solution was heated slowly to 50 °C under magnetic stirring, and then ammonia water (2.5 mL) was added into the solution. Afterwards, tetraethyl orthosilicate (TEOS, 4 g) was added dropwise into the stirred suspension to react at 50 °C for 2 h. Stirring was lasted for 2 h and then the solution was centrifuged and washed with distilled water, followed by vacuum drying at 60 °C overnight. Finally, the solid product was calcined with a heating rate of 1 °C/min to 550 °C and then was kept for 5 h to obtain hollow silica nanospheres (HSNs).

HSNs were functionalized by the impregnation method with diethylenetriamine (DETA). A certain amount of DETA was dissolved in methanol and stirred for 30 min at ambient temperature. Then, silica nanospheres synthesized were added and the solution was stirred for 10 h at ambient temperature. The products were dried in an oven at 60 °C for 5 h, and dried again under vacuum at 50 °C for 10 h. The powder obtained was named as DETA-HSNs. Finally, DETA-modified HSNs with a desired amount were dispersed into DMEE, and the absorbents named as DETA-HSNs/DMEE were obtained.

2.2 Characterization of materials

To comprehensively understand and analyse the physicochemical properties, various characterization techniques were adopted. scanning electron microscopy (SEM) images of surface topography of silica nanospheres were obtained using a field emission scanning electron microscope (Tecnai G2 F20, USA). Transmission electron microscopy (TEM) images were recorded by a transmission electron microscope (JEM 1200EX, Japan). The powdered samples for the TEM measurements were suspended in ethanol and then the mixed solution was dropped onto the Cu grids with holey carbon films the isotherms. N₂ adsorption-desorption isotherms at 77 K were acquired in a Micromeritics ASAP 2010 instrument. Before each isotherm experiment, degasification was performed for 5 h at 423 K in vacuum for samples without modification and 8 h at 393 K for samples modified by amines. The surface areas of samples were calculated using a Brunauer-Emmett-Teller (BET) model, and their pore distributions were calculated using a Density Functional (DFT) model. To analyse the chemical bonds of samples and verify the success of amino loading, Fourier-transform infrared spectroscopy (FTIR) analysis was performed using a Thermal NEXUS spectrometer (Thermo Scientific), and the spectra of samples were recorded in the 4,000 - 400 cm⁻¹ region.

2.3 CO₂ absorption-desorption

As shown in Figure 1, a dual-vessel absorption system is set up to investigate the performance of synthesized absorbents for CO₂ absorption. It consists mainly of a gas reservoir, a vacuum pump, a stainless steel absorption vessel (20 mL) with a magnetic stirrer, a water bath (a control precision of temperature, 0.5 K), a vacuum pump, pressure sensors with an accuracy of 0.32 kPa in the experimental pressure range, and a set of data acquisition equipment.

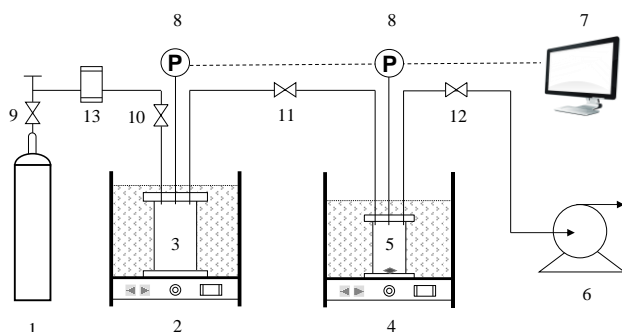


Figure 1: Schematic illustration of CO₂ absorption-desorption system (1: CO₂ cylinder; 2, 4: magnetic stirrers with thermostatic water bath; 3: gas reservoir; 5: absorption vessel; 6: vacuum pump; 7: data acquisition equipment; 8: pressure sensor; 9, 10, 11, 12: valve)

In each experiment, absorbent of about 5 g is weighed and placed into the absorption vessel. The experimental procedure is shown in previous work (Ding et al., 2018). The amount of CO₂ absorbed can be calculated using the following Eq(1):

$$n_{CO_2} = \frac{P_0 V_R - P(V_R + V_A - V_L)}{M_L R T} \quad (1)$$

Where V_R , V_A and V_L denote the volumes of storage vessel, absorption vessel and the absorbent, respectively. M_L represents the mass of the absorbent. P represents the saturated vapour pressure of liquid, and P_0 is the initial pressure in the storage vessel. To evaluate the experimental system error, the uncertainty analysis of ± 0.0849 mmol/g about CO_2 capacity was calculated by the error propagation law.

3. Results and discussion

3.1 Characterization of materials

Figure 2 presents the SEM and TEM images of HSNs. As illustrated in the SEM images (Figure 2(a) and (b)), HSNs possess mono-dispersed and uniformed sphere-like morphology with a few silica nanoparticles attaching to the outer surface of the spheres. TEM image can further indicate the information of internal structure in these spheres. The dark shells and bright cores can be obviously distinguished in Figure 2(c), indicating the internal hollow structure of HSNs (Gao et al., 2018). The inner hollow structure is also revealed by some broken hollow spheres in SEM images. Moreover, HSNs has a diameter of approximately 220 nm, with same shell thicknesses of approximately 14 nm. To further investigate the crystal structure of HSNs, a strong diffraction peak appear at $2\theta = 0.31^\circ$ in the small-angle XRD spectrum (Figure 3), indicating that ordered pore structures exist in the samples.

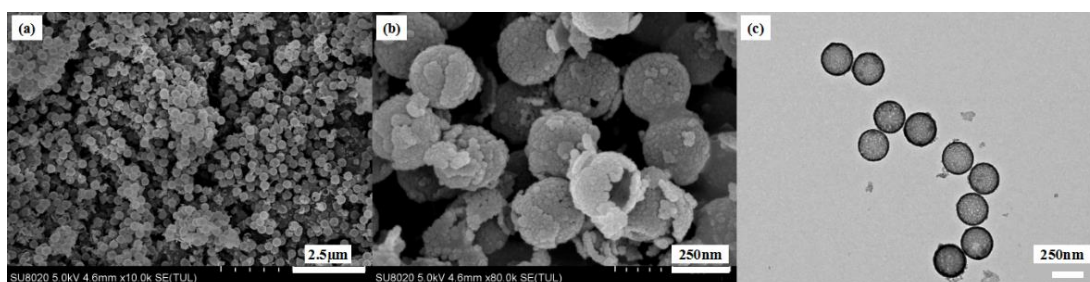


Figure 2: SEM images (a), (b) and TEM image (c) of HSNs

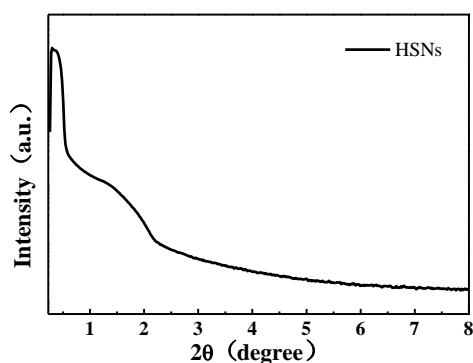


Figure 3: Small-angle XRD of HSNs

Surface area and porosity analysis is used to investigate the properties of porous structure. Figure 4 shows the nitrogen adsorption-desorption isotherms and pore size distribution curve of HSNs. As shown in Figure 4(a), HSNs displays type IV isotherm with hysteresis loops of H3-type in the region of higher relative pressure. The primary reason is that capillary condensation occurred in the pores of the shell formed from the broken hollow spheres (Wang et al., 2017). The porous structure parameters are calculated, and the specific surface area, pore volumes and average pore size of samples are 230.95 ± 1.66 m²/g, 0.7576 m³/g and 11.71 nm, respectively. Figure 4(b) shows the pore size distributions of HSNs calculated by DFT model. Two sharp and narrow peaks at around 1.49 nm and 2.76 nm represent microporous region and mesoporous region, respectively. However, the dV/dD value of the peak in microporous region is much larger than that in mesoporous region, which indicates that HSNs possess porous structures dominated by micropores.

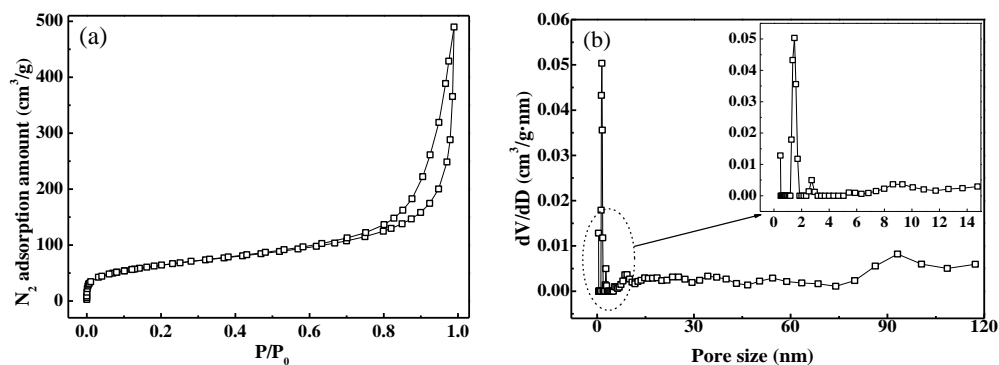


Figure 4: (a) Nitrogen adsorption-desorption isotherms and (b) pore size distribution of HSNs

Figure 5 displays the FTIR spectrum of HSNs before and after DETA impregnation. For two samples, due to the Si-O-Si asymmetric stretching, a sharp and intense peak appears in the region of 1,000 - 1,300 cm^{-1} is associated with the asymmetric stretching vibrations of Si-O-Si band. For DETA-HSNs, two new peaks at 1,570 cm^{-1} and 1,481 cm^{-1} are the characteristics of the asymmetric and symmetric vibrations of N-H from the primary amine (-NH₂) in DETA. The peak at about 1,318 cm^{-1} is assigned to C-N bending mode (Cecilia et al., 2016). The characteristics of DETA and silica shown in FTIR spectra imply that DETA is impregnated well in silica nanospheres.

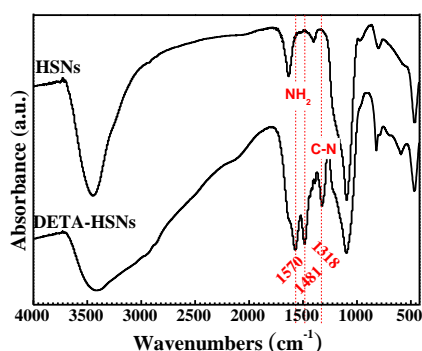


Figure 5: FTIR analysis of HSNs and HSNs modified by DETA

3.2 CO₂ absorption

Based on the DMEE and hollow silicon nanospheres modified by DETA, a kind of novel absorbents was obtained, called as DETA-HSNs/DMEE. The CO₂ absorption performance of the absorbents with different amount of DETA were investigated. Here, a concept of rapid absorption time is defined as the time taken for 90 % saturated absorption capacity. Figure 6(a) shows the CO₂ absorption curves of DETA-HSNs/DMEE based nanospheres with different DETA loading contents at 27 °C and 150 kPa. Two stages can be observed, namely rapid absorption stage and slow absorption. In this paper, the rapid absorption stage is considered as the process when the absorption amount of CO₂ reaches 90 % of the saturated absorption amount. Then the slow absorption stage follows, where carbon dioxide molecules first diffuse to the acting sites in the pores and then react with DETA loaded on the wall of inner pores. Hence, the mass transfer rate of carbon dioxide in pores plays a decisive role in the slow absorption stage. In the experiments, it is observed that part of amines could not be loaded on HSNs, when the DETA content is larger than 60 wt%. Hence, a DETA content range of 0 - 60 wt% was selected to investigate the effect of DETA content on CO₂ absorption performance. As shown in the Figure 6(a), the more DETA content will lengthen the slow absorption stage and decreases the absorption rate. That may be because the more amines fill the pore in the spheres, resulting in a decrease of pore sizes and a greater resistance of CO₂ transfer.

To further reveal the effect of DETA load on the CO₂ absorption performance of absorbents, Figure 6(b) shows the CO₂ absorption amounts and absorption times of DETA-HSNs/DMEE with different DETA contents. As the DETA loading content increases from 0 to 60 wt%, the CO₂ absorption amount increases from 0.4390 ± 0.0849

mmol/g to 1.0630 ± 0.0849 mmol/g, due to more amino could react with CO_2 . However, the time required is lengthened from 37 min to 72 min.

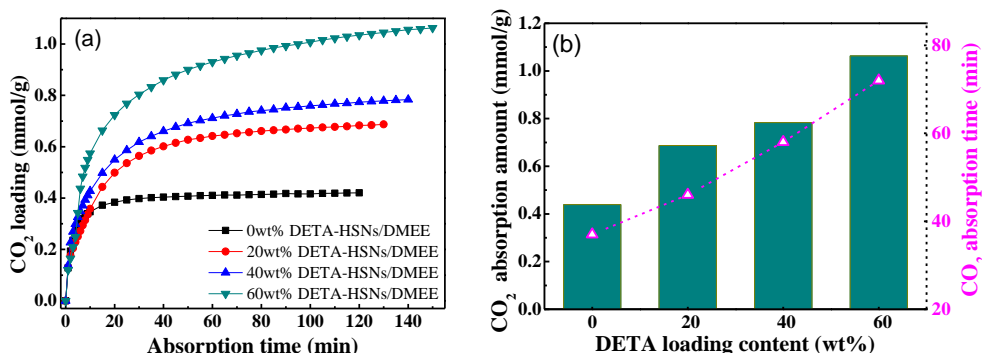


Figure 6: (a) Absorption curves of DETA-HSMs/DMEE with different DETA content; (b) CO_2 absorption amounts and apparent absorption rates at 25 °C and 150 kPa.

3.3 Absorption kinetic models

To thoroughly explore the mechanism of CO_2 transfer process in three absorbents samples, pseudo-first-order and pseudo-second-order were adopted to further analyze the experimental results and their linear forms could be expressed as follows (Liu and Yu, 2018):

$$\ln(q_e - q_t) = \ln q_e - k_1 t \quad (2)$$

$$\frac{t}{q_t} = \frac{1}{k_2 q_e^2} + \frac{t}{q_e} \quad (3)$$

where q_e and q_t (mmol/g) are the amount of CO_2 absorbed at equilibrium and any time t (min); k_1 (min^{-1}) and k_2 ($\text{g mmol}^{-1} \text{min}^{-1}$) are pseudo-first-order and pseudo-second-order adsorption rate constants.

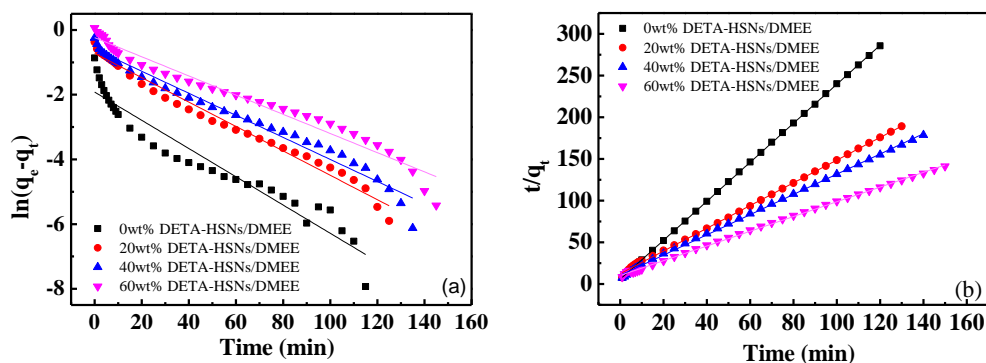


Figure 7: Fitting of absorption kinetic models of CO_2 absorption in DETA-HSNs/DMEE: (a) pseudo-first-order model; (b) pseudo-second-order model

Figure 7 shows the relationship of $\ln(q_e - q_t)$ versus t for pseudo-first-order model and the relationship of t/q_t versus t for pseudo-second-order model, and the approximated values of k_1 , k_2 , q_e and corresponding coefficients of determination R^2 calculated by linear regression are listed in Table 1. Comparing with the pseudo-first-order model, it can be easily found that q_e values calculated by pseudo-second-order model are more close to the experimental q_e , and the R^2 values of pseudo-second-order model are higher than those of pseudo-first-order model. It indicated that pseudo-second-order model could be successful to predict the CO_2 absorption process in the colloidal suspensions studied in this work, due to the primary chemical reaction. Interestingly, a larger value of k_2 is obtained in absorbent without amino load. With the increase of DETA loading content, the values of k_2 for DETA-HSNs/DMEE display a marked decrease.

Table 1: Kinetic model parameters for CO₂ absorption in DETA-HSNs/DMEE

Samples	$q_{e,exp}$	Pseudo-first order			Pseudo-second order		
		$q_{e,cal}$	k_1	R^2	$q_{e,cal}$	k_2	R^2
0wt% DETA-HSNs/DMEE	0.4390	0.1468	0.0437	0.9295	0.4274	0.9852	0.9999
20wt% DETA-HSNs/DMEE	0.6870	0.4861	0.0377	0.9851	0.7336	0.1522	0.9993
40wt% DETA-HSNs/DMEE	0.7835	0.5523	0.0341	0.9768	0.8246	0.1412	0.9992
60wt% DETA-HSNs/DMEE	1.0630	0.7902	0.0296	0.9671	1.1316	0.0764	0.9992

4. Conclusions

In summary, hollow silica nanospheres with uniformity and excellent dispersibility were synthesized successfully, and can be used as a good support of DETA. HSNs possess porous structures dominated by micropores. In addition, the novel sorbent was prepared by suspending DETA-HSNs in DMEE. The CO₂ absorption experiments indicates that DETA loading on HSNs can obviously enhance the CO₂ absorption capacity. With the DETA content increasing from 0 to 60 wt%, the CO₂ absorption capacity can increase to 1.0630 ± 0.0849 mmol/g at the temperature of 27 °C and the pressure of 150 kPa, while more DETA will fill the pore in the spheres and increase resistance of CO₂ transfer during the slow absorption stage. The fitting of absorption kinetic models of CO₂ absorption in DETA-HSNs/DMEE shows that pseudo-second-order model is more successful to predict the CO₂ absorption process in the colloidal suspensions. In the future research, the comprehensive absorption/desorption performance need to be studied and improved, and the mechanisms of CO₂ absorption in the anhydrous colloidal suspension will be explore further.

Acknowledgments

We gratefully acknowledge the financial supports by National Natural Science Foundation of China (No. 51876013 and No. 51576022), and the Fundamental Research Funds for the Central Universities (2018CDXYDL0001).

References

- Amir, D., Mojtaba, R., Abouzar, A., Alireza, B., Mohammadi, A.H., Morteza, A., 2018, Rigorous prognostication and modeling of gas adsorption on activated carbon and zeolite-5a, *Journal of Environmental Management*, 224, 58-68.
- Cecilia J.A., Vilarrasa E., García C., Saboya R.M.A., Azevedo D.C.S., Cavalcante C.L., 2016, Functionalization of hollow silica microspheres by impregnation or grafted of amine groups for the CO₂ capture. *International Journal of Greenhouse Gas Control*, 52, 344-356.
- Ding Y.D., Li X.Q., Guo L.H., Liao Q., Zhu X., 2018, Synthesis of colloidal suspension based on porous silica nanospheres and its CO₂ absorption, *Chemical Engineering Transactions*, 70, 1657-1662.
- Gao Y., Ding S., Huang X., Fan Z., Sun J., Hai Y., 2018, Development and evaluation of hollow mesoporous silica microspheres bearing on enhanced oral delivery of curcumin, *Drug Development and Industrial Pharmacy*, 1-27.
- IEA, 2017, *Energy Technology Perspectives 2017*, <<https://www.iea.org/etp2017/summary/>> accessed 02.10.2018.
- Jiao J., Cao J., Xia Y., Zhao L., 2016, Improvement of adsorbent materials for CO₂ capture by amine functionalized mesoporous silica with worm-hole framework structure, *Chemical Engineering Journal*. 306, 9-16.
- Ling H., Liu S., Gao H.X., Liang Z.W., 2019, Effect of heat-stable salts on absorption/desorption performance of aqueous monoethanolamine (MEA) solution during carbon dioxide capture process, *Separation and Purification Technology*, 212, 822-833.
- Liu Y.M., Yu X.J., 2018, Carbon dioxide adsorption properties and adsorption/desorption kinetics of amine-functionalized kit-6. *Applied Energy*, 211, 1080-1088.
- Mehassouel A., Derriche R., Bouallou C., 2016, A New CO₂ Absorption Data for Aqueous Solutions of N-methyldiethanolamine plus Hexylamine, *Chemical Engineering Transactions*, 52, 595-600.
- Nie L.J., Mu Y.Y., Jin J.S., Chen J., Mi J.G., 2018, Recent developments and consideration issues in solid adsorbents for CO₂ capture from flue gas, *Chinese Journal of Chemical Engineering*, 26, 2303-2317.
- Rezaeian M., Izadyar M., Nakhaei P.A., 2018, Carbon Dioxide Absorption by the Imidazolium-Amino Acid Ionic Liquids, Kinetics, and Mechanism Approach, *The Journal of Physical Chemistry A*, 122, 5721-5729.
- Wang D., Li X., Liu Z., Shi X., Zhou G., 2017, Preparation of hollow silica nanospheres in O/W microemulsion system by hydrothermal temperature changes. *Solid State Sciences*, 63, 62-69.